Titel: MCF lab report on METIS experiments
Name: Tobias Schuett
Email: tms535@york.ac.uk
Full Analysis: github.com/tobiasschuett/mcf-lab

Remark: This document explains the methods used and presents and discusses the obtained results for all METIS experiments. For details of how the coding and analysis was actually performed in detail please refer to the print out of the file `metis_analysis.ipynb` and `metis_analysis2.ipynb` available at the Github address given above.

Contents

1 Power injection and H-mode

1.1 Method

METIS was run with the default file and the mulitplier of both NBI injections was changed by the same amount. The simulation result was saved as a .mat file and average data

(also the NBI power) for each shot was obtained by averaging during the flattop as shown in figure 1. This was done such that total NBI powers from 0-40MW were covered. The parameters of interest H-mode indicator, electron density, electron temperature, pressure beta, confinement time were extracted and the triple product calculated from these. The result can be seen in section 1.2. The uncertainties of each datapoint is given by the standard deviation that results from the averaging during the flattop.

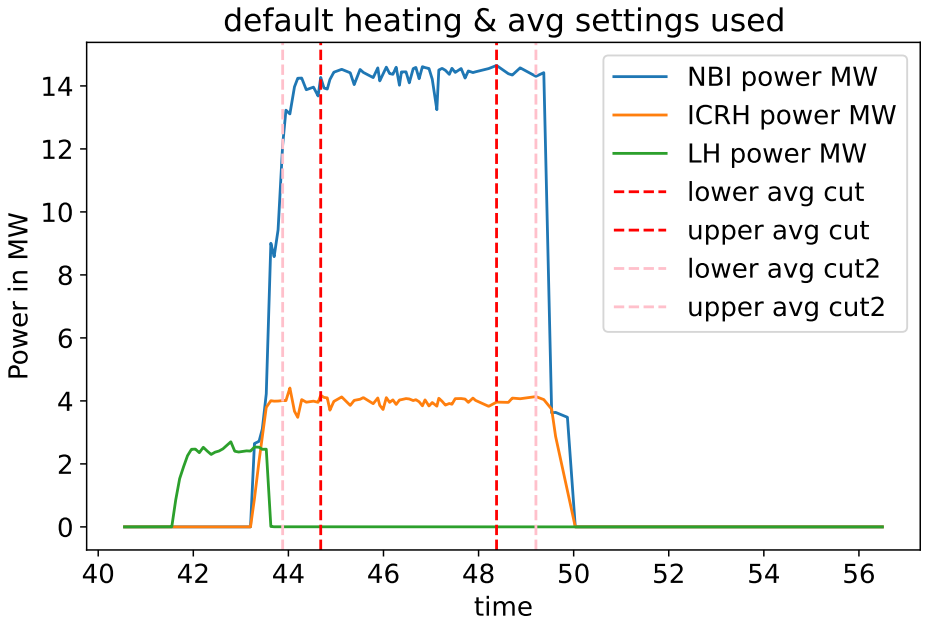

Figure 1: The flattop of the default file indicating where the averaging section is. Section 1.2 uses the "cut" interval.

1.2 Result

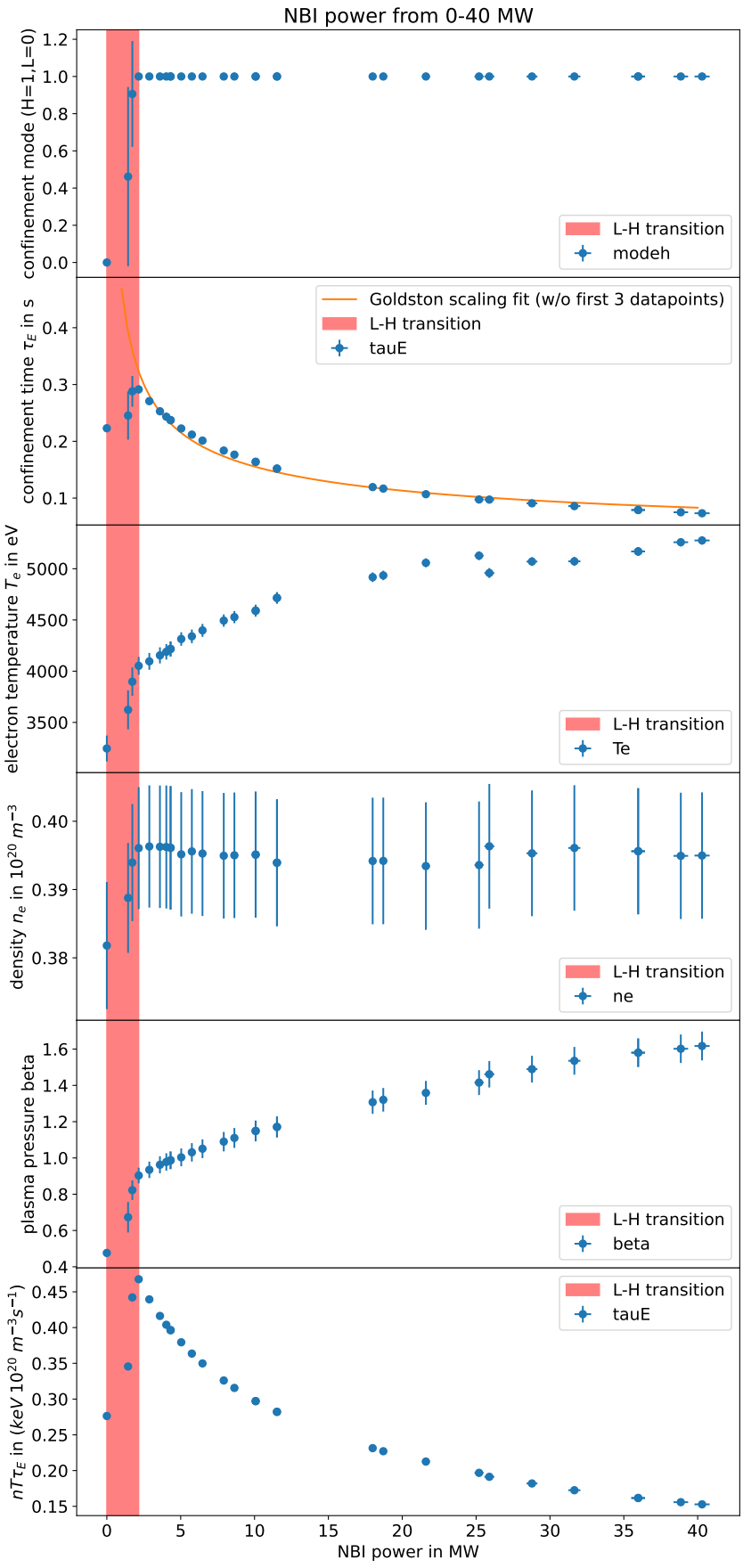

Figure 2: Results of all average values of parameters during flattop for NBI powers 0-40MW.

1.3 Discussion

The triple product follows the general trend of the confinement time, i.e. peaks at $\sim$ 4.68 10^{19} keV/m^3/s and then decreases with increasing NBI power in H-mode. This is about two orders of magnitude lower than the ignition requirement of $> 5\ 10^{21}$ keV/m^3/s [1, p.12].
The electron density shows to increase signifantly before L-H transition and then stays roughly constant once in H-mode. Plasma beta which is proportional to pressure given our constant magnetic field, as well as temperature show to increase in H-mode, however with decreasing slope. *In general it can be noted that the most drastic changes happen during and before the transition to H-mode, just as expected.*
It can be seen that once in H-mode, the confinement time decreases with increasing Power even though H-mode is maintained. This is known as confinement degradation and the accepted scaling is given by the Goldston scaling [2]. The Goldston scaling is based on L-mode data but since confinement degradation persists in H-mode and scaling has been shown to be similar [3]. given by $\tau_E \propto I_p P_{tot}^{-0.5}$ (The rest is major minor radius and elongation, all geometrical and fixed here). Since $I_p \approx const.$ during flattop (see beginning figures), we can fit $\tau_E \propto c_1 P_{NBI}^{-0.5} + c_2$ where c_2 captures all the other power input. Fit shown in first graph and shows to agree well with trend of data (Note that first 3 datapoints of L-H transition have been omitted for fit).

2 Access to H-mode

2.1 Effect on confinement time and triple product by B_t,I_p and $\overline{n_e}$

2.1.1 Method

Analogous to the scan of NBI powers in section , the multipliers of toroidal magnetic field B_t, plasma current I_p and avg electron density $\overline{n_e}$ were varied and each simulation saved as .mat file and parameters of interest averaged over the flat top. Note that for all I_p and $\overline{n_e}$ it is possible to also extract their change, while this does not work for B_t. Hence B_t is given in arbitrary units.

2.1.2 toroidal field

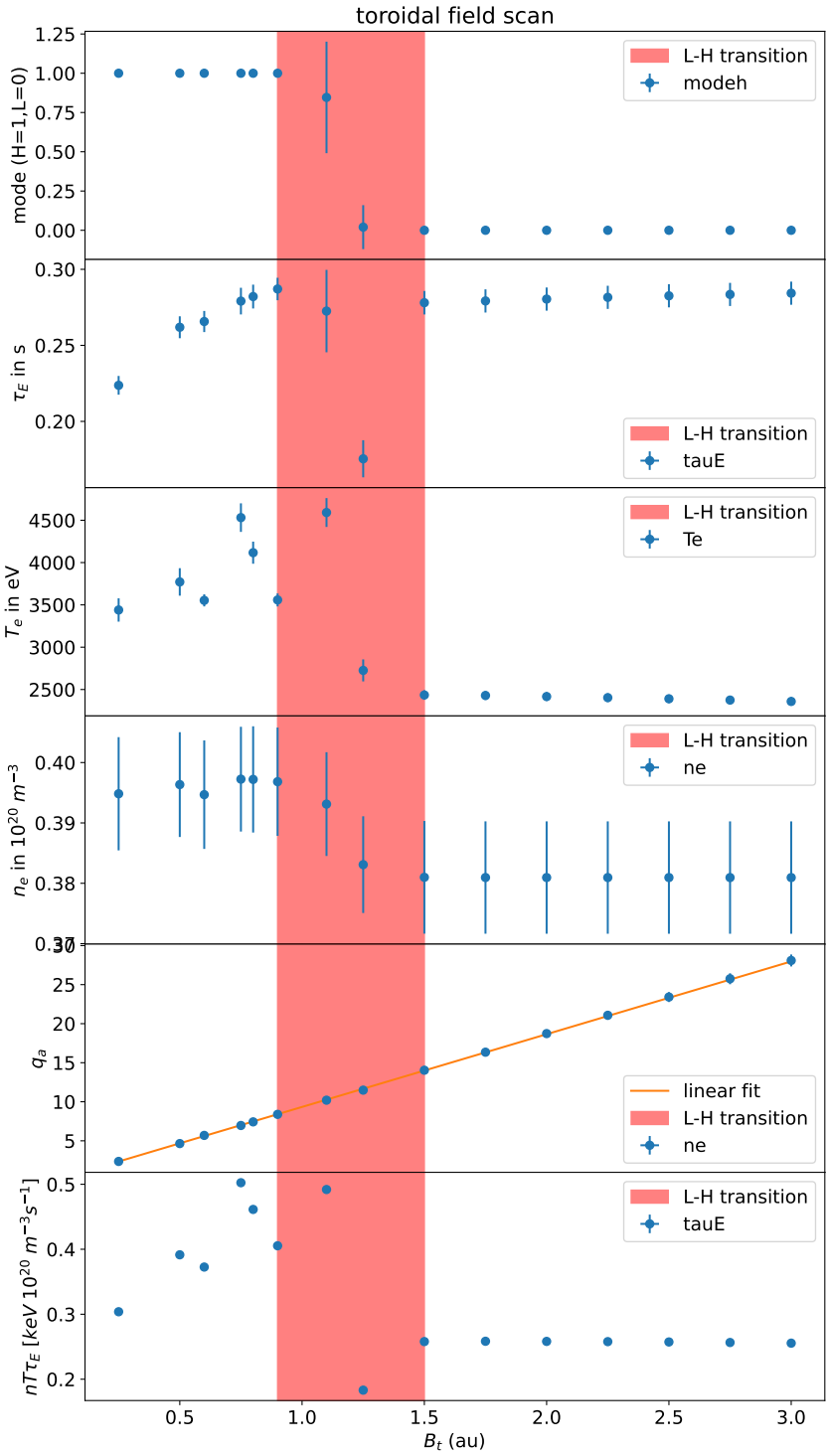

Figure 3: The confinement parameters for varying toroidal magnetic field.

The results in figure 3 show that the triple product increases in H-mode with increasing B. At some critical B_t the plasma goes into L-mode and stays in L-mode with increasing B. We shall see later that this caused by the fact that L-H transition threshold increases in B, hence the threshold is not reached for higher B due to constant heating power. In the graphs of n,T and τ_E we see that it is mostly the temperature and the density that

drop, not the confinement time.
The edge safety factor q_a shows to linearly increase in B_t. The safety factor is defined as the number of toroidal turns that are necessary for one full poloidal turn. In the cylindrical approximation this becomes [4, p.287]:

$$q_a = \frac{aB_z}{RB_\theta} = \frac{2\pi a^2 B_z}{R\mu_0 I_p} \tag{1}$$

approximating $B_t \approx B_z$, we expect a linear relationship between edge safety factor and toroidal field. The simulation data in 3 shows to match this expectation.

2.1.3 plasma current

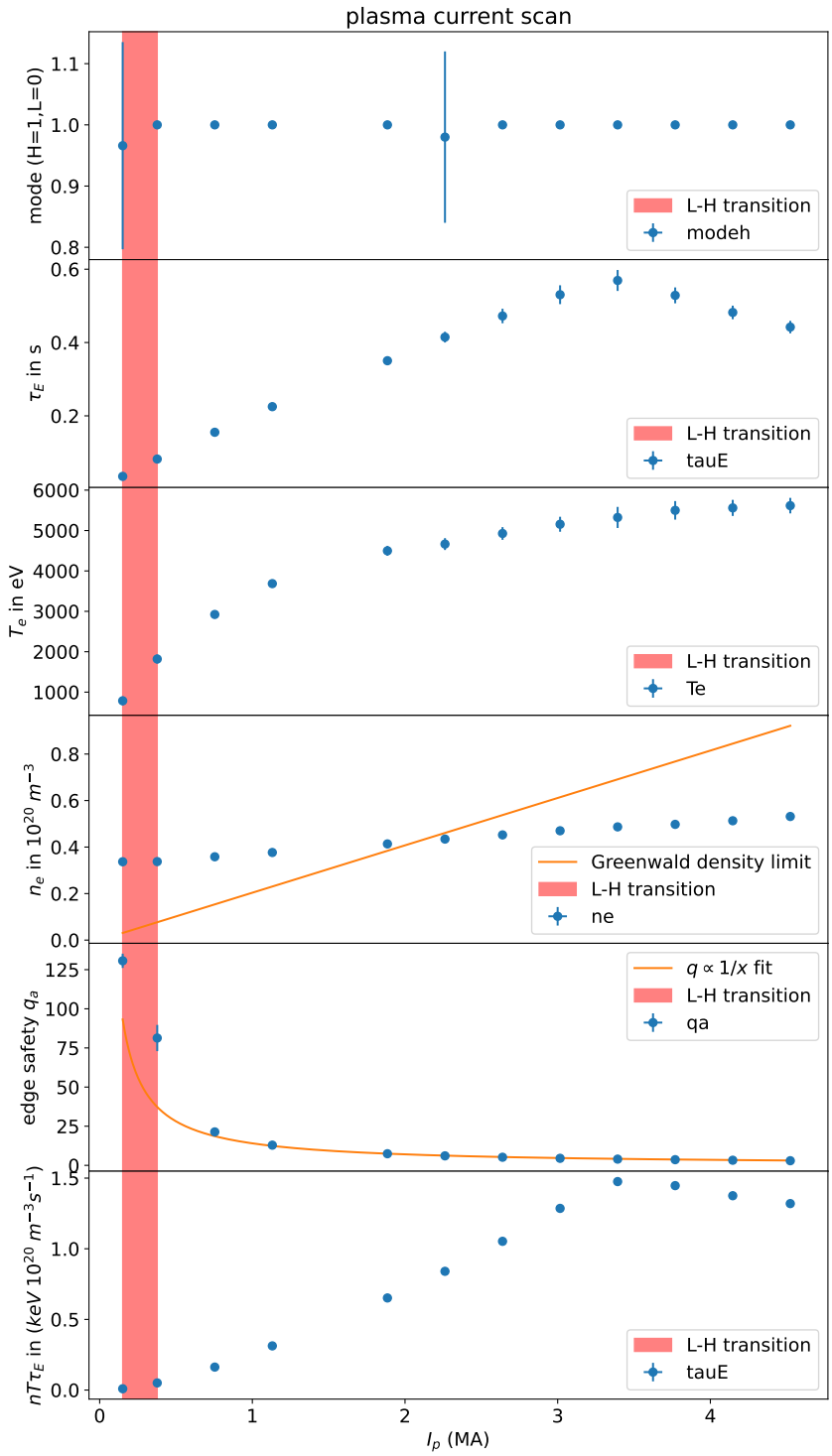

Figure 4: The confinement parameters for varying plasma current.

The measurements in figure 4 here basically only capture H-mode behaviour. The triple product shows to increase with increasing plasma current in H-mode up to some critical current $I_{p,max} = (3.39 \pm 0.02)$ MA, after which the triple product drops again. Plots of n,T and τ_E show that this behaviour of the triple product is caused by a peak in confinement time.

Figure 4 also shows that as the average density crosses the Greenwald density limit [5], the confiment mode indicator at the top of the figure has a very large uncertainty and is not exactly equal to unity. This uncertainty from oscillating values of H-mode and L-mode during the flattop, i.e. a unstable confinement configuration as predicted by this density limit. However, unexpectedly the results also show that the simulation outputs a stable plasma configuration in H-mode even for densities larger than n_G.
The edge safety factor q_a data in figure 4 shows to match the expected "1 over x" behaviour from equation 1 for data points in H-mode.

2.1.4 average electron density

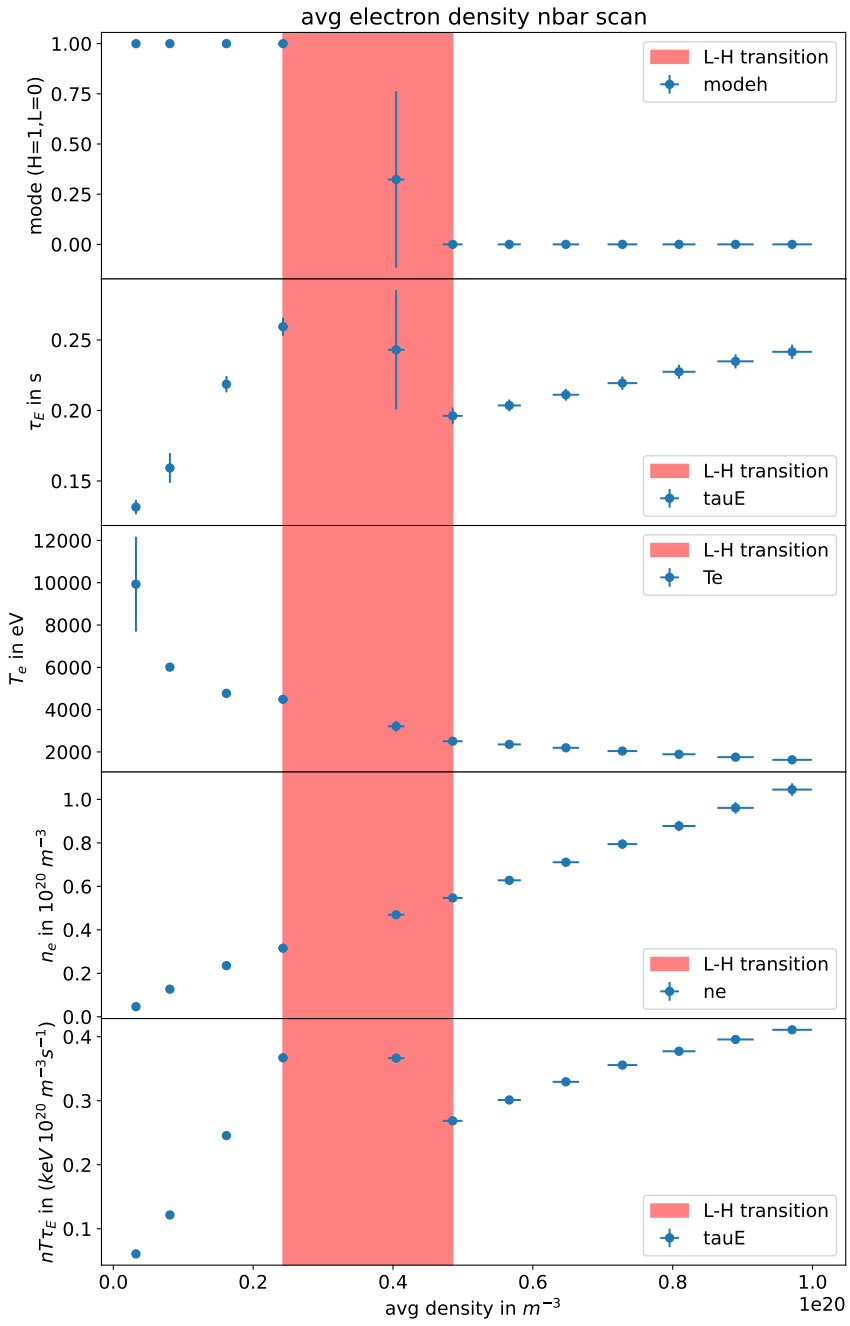

Figure 5: The confinement parameters for varying average electron density.

Figure 5 shows that the triple product increases with density in H-mode, then drops as the plasma is in L-mode with increasing density. We will show later that this due to higher threshold with increasing density and heating is constant here. In L-mode, the triple product also increases with increasing density. Looking at the individual plots shows that this behaviour is mostly caused by confinement time. It makes sense for τ_E to generally increase with average density. A higher average density means a higher particle confinement time τ_N. If the avg energy of particles that are lost does not change significantly as τ_N increases, that means that fewer particles being lost corresponds to less energy being lost, i.e. a higher τ_E.

2.2 L-H transition power threshold as a function of B_t and $\overline{n_e}$

2.2.1 Method

For different toroidal field settings the total NBI power was increased (still over separate shots) from 0-14MW to capture the L-H transition known from results before to happen in this region. The H-mode indicator paramter was averaged along the flattop for each of these shots allowing one to create a plot of "avg H-mode indicator" against toroidal field. The result of this is shown in figure 6. The analogous procedure was performed for varying average density and is shown in figure 7.

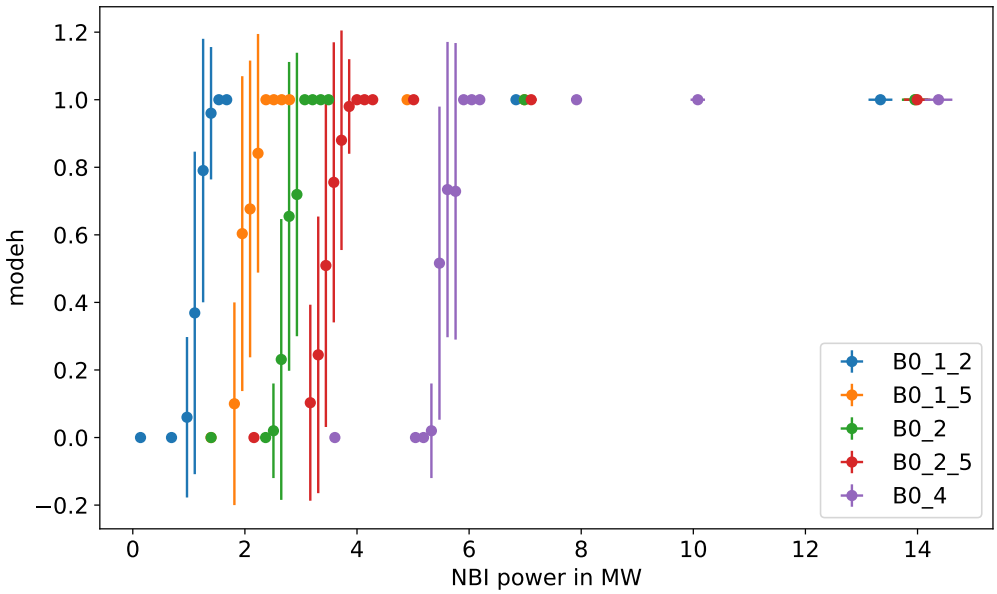

Figure 6: The average H-mode indicator against total NBI power for different toroidal fields. This is the data from which P_{LH} can then be determined for each toroidal field

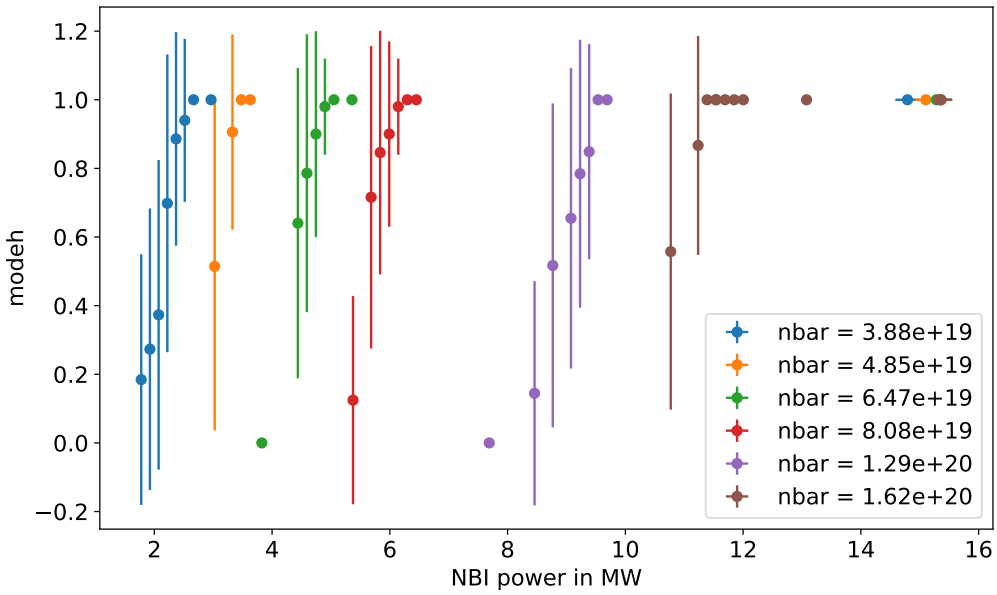

Figure 7: The average H-mode indicator against total NBI power for different avg densities. This is the data from which P_{LH} can then be determined for each avg density.

Using the data in figure 6 the L-H transition threshold power was set as the first data point for which the avg H-mode indicator is equal to unity. The uncertainty of this threshold power is then given by the average distance between the neighbouring data points[1].

2.2.2 Results

The results for the L-H threshold power against toroidal filed was obtained as described in section 2.2.1 and shown in figure 8. The L-H threshold dependence on avg density is shown in figure 9.

[1] As the spacing is approximately equal, I have neglected using an asymmetric uncertainty interval.

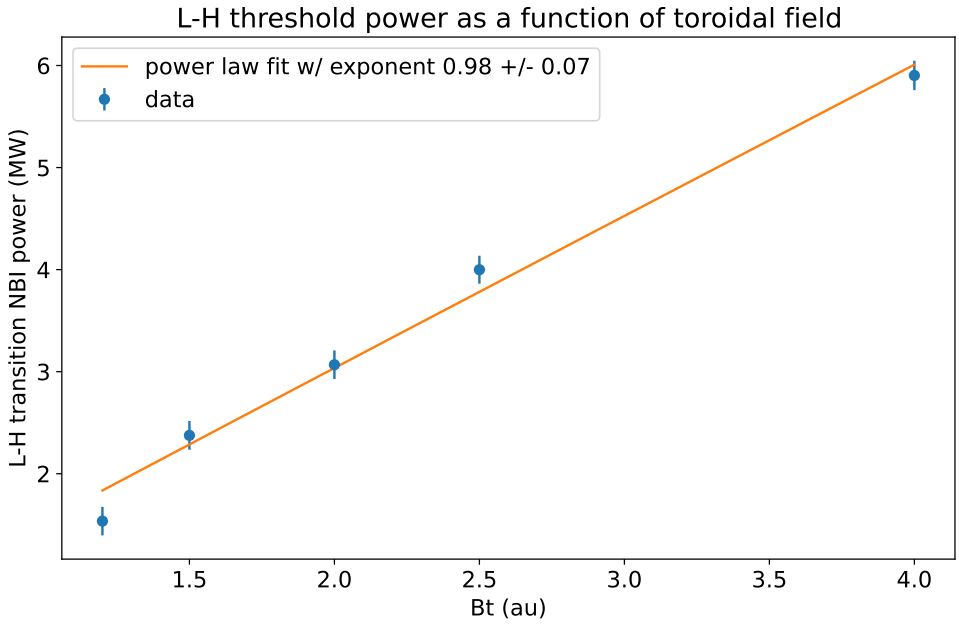

Figure 8: The L-H threshold dependence on toroidal field obtained from figure 6

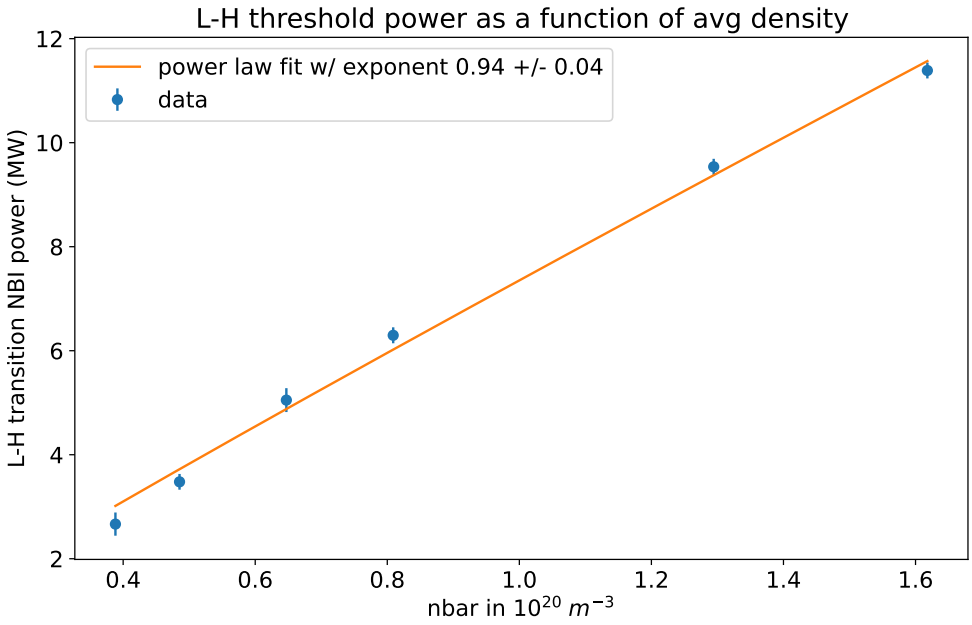

Figure 9: The L-H threshold dependence on avg density obtained from figure 7

The results in figure 8 and 9 show that $P_{LH} \propto \bar{n_e}^{0.94\pm0.04} \bar{B_t}^{0.98\pm0.07}$. The widely accepted empirical Martin's scaling from 2008 based on 1024 time slices (of which 562 stem from JET) [6, p.3] which states that $P_{LH} \propto \bar{n_e}^{0.717\pm0.035} \bar{B_t}^{0.803\pm0.032}$. We not that the exponent intervals do not overlap, however a scaling exponent close to but below unity is captured here as well.
In general this scaling of course means that increasing the density for higher fusion reaction

rate as well as increasing the toroidal magnetic field for higher pressure at constant beta and therefore higher fusion reaction (if T constant) both requires a higher initial power threshold that the heating system must deliver to even enter H-mode in the first place.

2.3 Additional comment on safety factor

It should be noted that the minimum edge safety factor q_a in figure 3 and 4 is (2.36 ± 0.07) for B_t and (2.96 ± 0.09) for I_p. Hence the Kruskal-Shafranov limit of $q > 1$ against external kink modes is always satisfied and no disruptions are expected or observed. Furthermore, figure 10 shows the q factor never drops below unity anywhere in the plasma and hence the plasma is also expected to be free of internal kink modes that would lead to sawtooth instabilities in core electron temperatures.

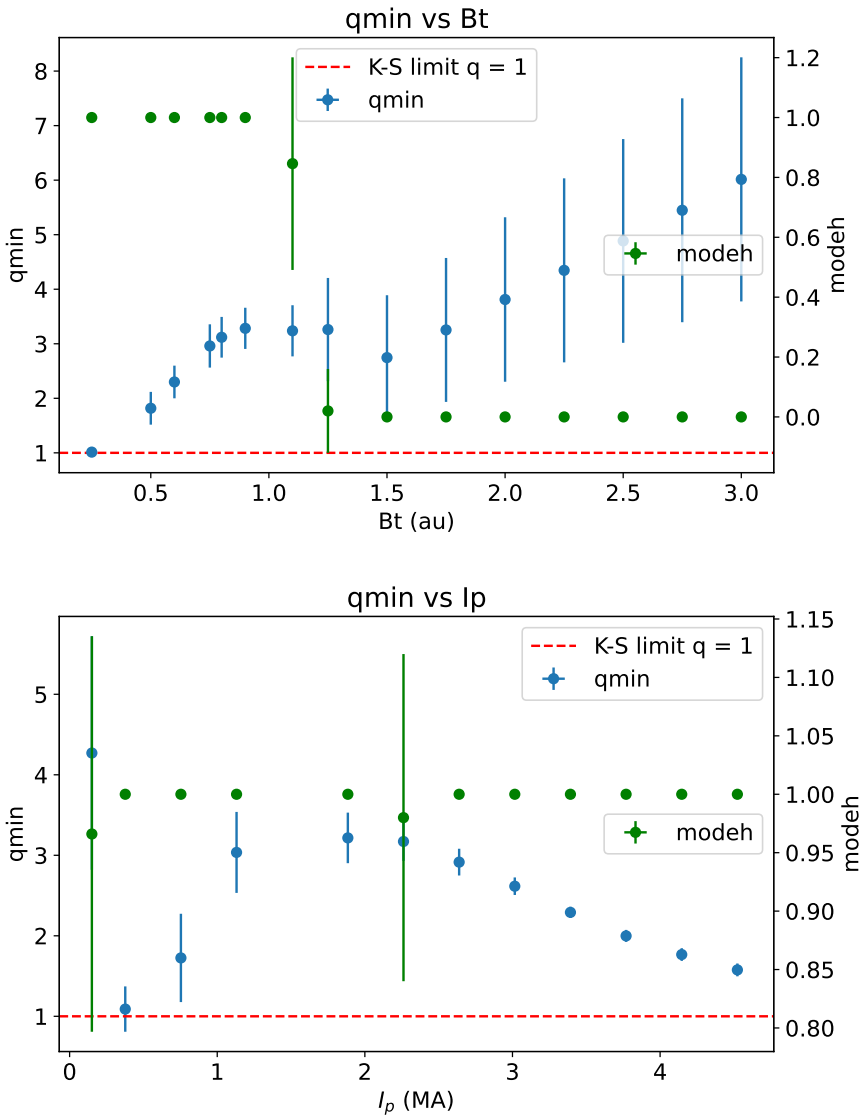

Figure 10: The minimal q value (radial) for each toroidal field and plasma current configuration.

3 Power ramp experiments

3.1 method

Five different power ramp experiments were performed. For the first 4, the power waveform of both NBI power injectors was set such that it increases linearly during the flattop in time. An example plot for the first ramp experiment, where the power is increased from 0-10 MW in one shot, is shown in figure 11. Notice that figure 11 also shows the averaging interval used here which is now "cut2" as opposed to "cut" which was used before and shown in figure 1. The second ramp experiment consisted of two shots, where the first shot ramps from 0-5MW and the second shot ramps from 5-10MW. Following that logic the third ramp experiment consists of 0-3,3-6,6-9MW and the fourth experiment of 0-2.5,2.5-5,5-7.5,7.5-10MW.
The 5th experiment was one aggressive ramp from 0-40MW in one shot.
The confinement time was then extracted for each NBI power (or for each point in time).

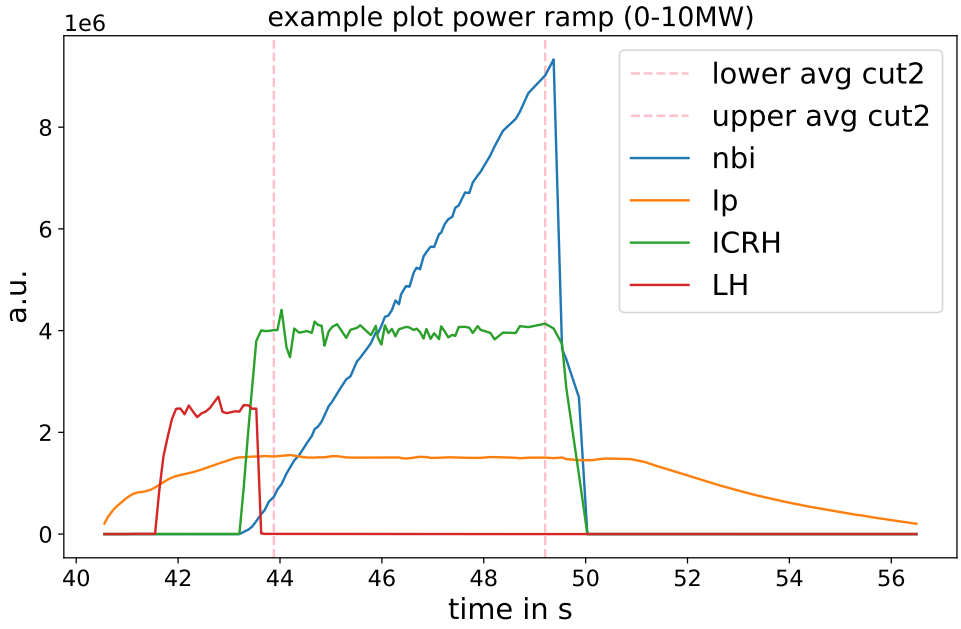

Figure 11: Example plot of NBI ramp showing the linear increase during the flattop. The interval used for the analysis is also shown in pink.

3.2 Results

The results of the first four ramp experiment in figures 12 and 13 show that the confinement time data generally clusters around the data from the static experiments from section 14. The data shows to differ significantly during the L-H transition. As the dynamic ramp experiment data generally transitions into H mode after the static data, this shows the lagging in adjustment of all parameters caused by the equilibrium calculation of METIS. The associated timescale for the power ramp is given by

$$\frac{1}{\tau} = \frac{1}{\overline{P}}\frac{dP}{dT} = \frac{1}{\overline{P}}\frac{\Delta P}{\Delta T} \tag{2}$$

where the last equality is true due to the linear ramp applied here. For the first four experiments $\overline{P} = 5$ MW,$\Delta P = 10$ MW and ΔT is given as multiples of the flattop time as 5.3s,10.6s,15.9s and 21.2s for ramp 1,2,3 and 4 respectively. Hence τ is given by 2.65s,5.3s,7.95s,10.6s for ramp 1,2,3 and 4, respectively. *For all 4 ramps this characteristic of the power ramp is more than one order of magnitude larger than the maximum confinement time.*
Using equation 2, the characteristic timescale for the agressive ramp shown in figure 14 is given by $\tau = 0.66$ s. This is on the order of the confinement time. This shows that even four fast increases the confinement time data stays close to the static data.
To quantify the error a power law relationship was fitted through the static H-mode data (hence omitting first 2 data points). This power law function was then used to calculate the average deviation and the residuals of the ramp data from the value expected based on the fit. The average deviation for data points of $P_{\mathrm{NBI}} > 3$ MW is given by 3.7%,2.4%,2.1%,2.5% and 2.3% for ramp 1-5, respectively.
The distribution of the residuals for ramp 1 and 2 are shown in figure 15 and for ramp 3-5 are shown in figure 16. *As the mean deviation/error stays approximately constant with increasing ramp speed, the residuals of ramp 1-4 show that the residual distribution seems to approach normality for slower power ramps.* The residuals of the aggressive ramp 5 show to be lower than expected.

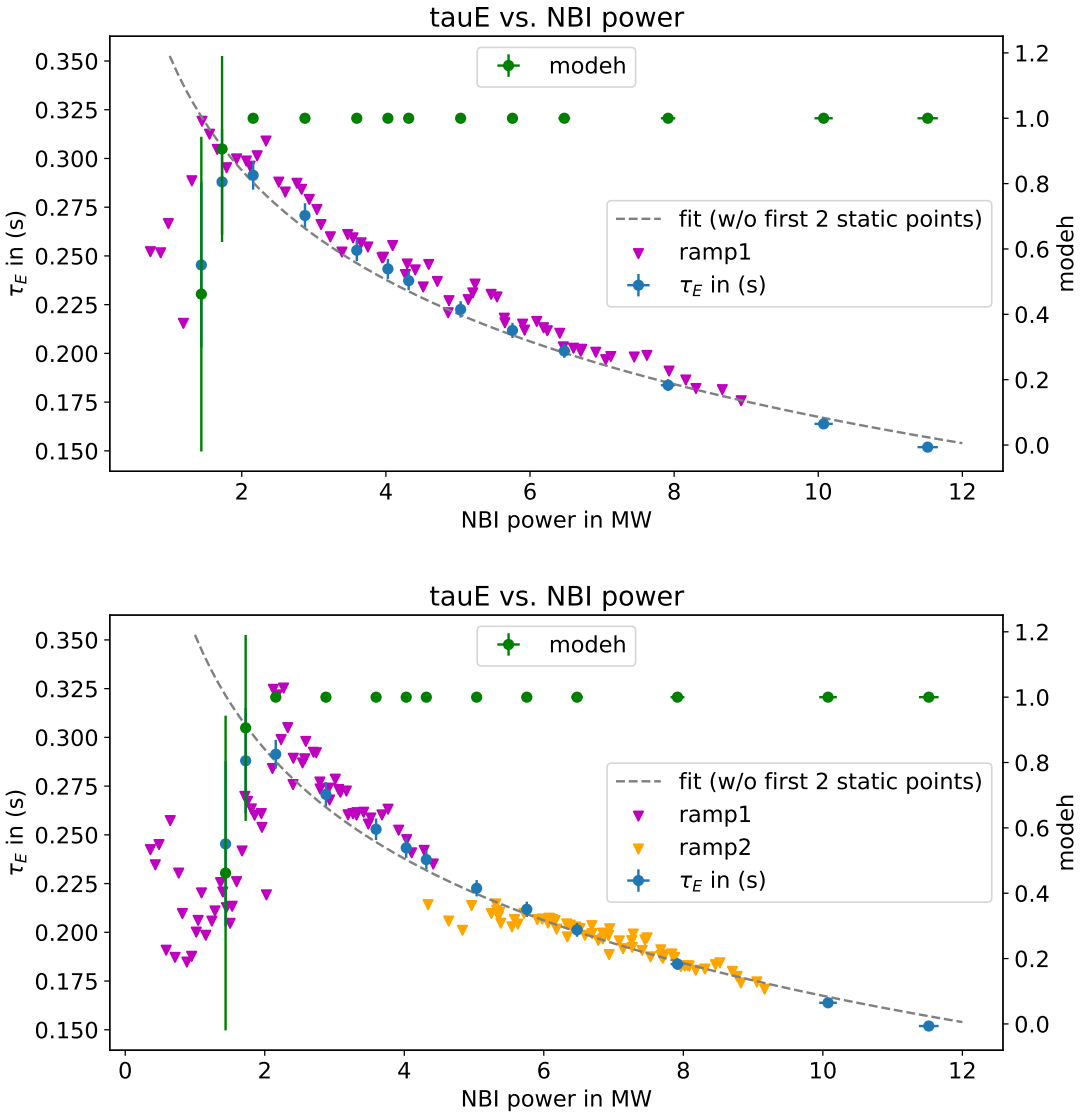

Figure 12: The confinement time against NBI power for the ramp experiments 1 & 2 compared to the static ramp data shown in blue here and taken from figure in section .

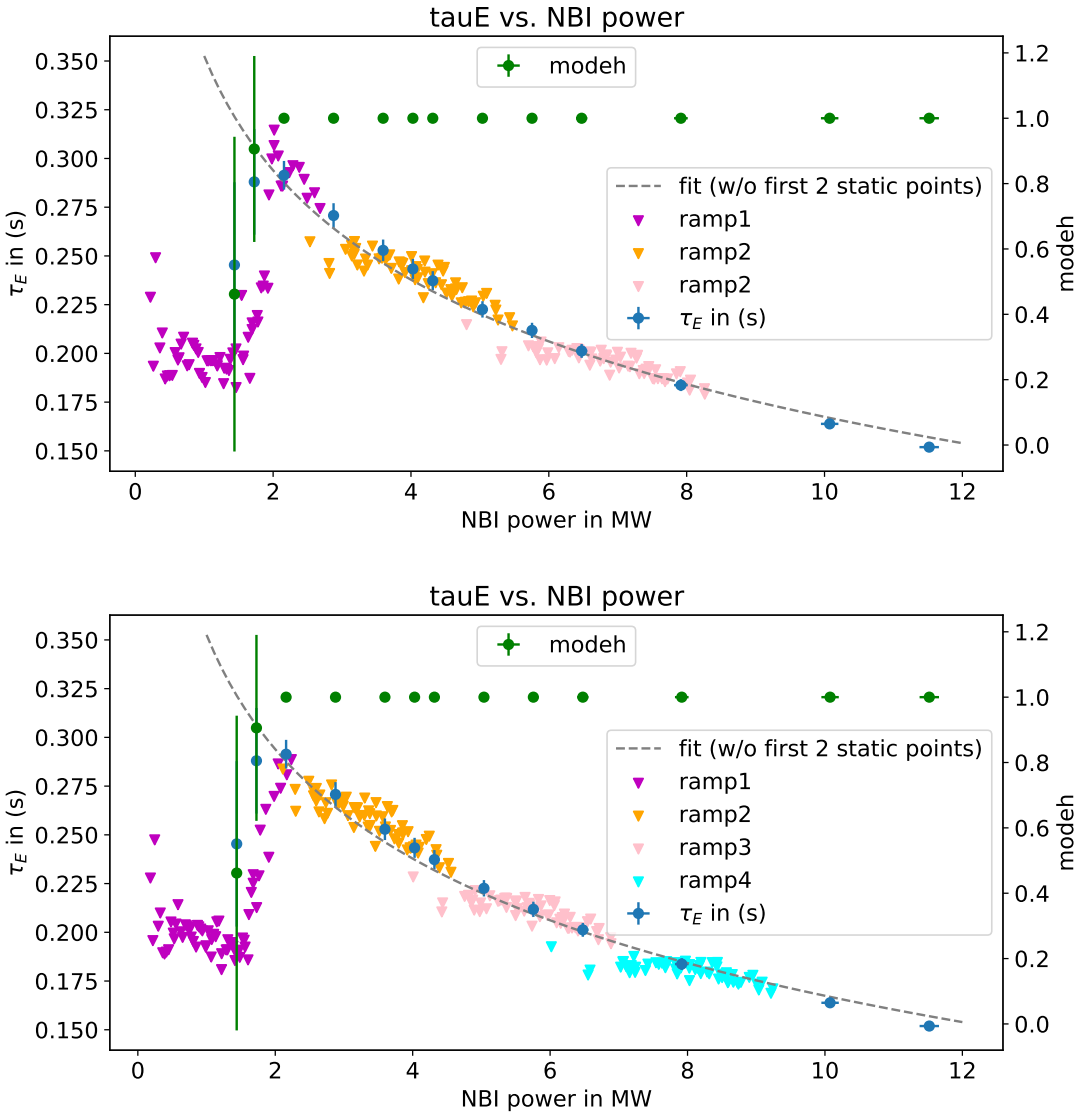

Figure 13: The confinement time against NBI power for the ramp experiments 3 & 4 compared to the static ramp data shown in blue here and taken figure in section .

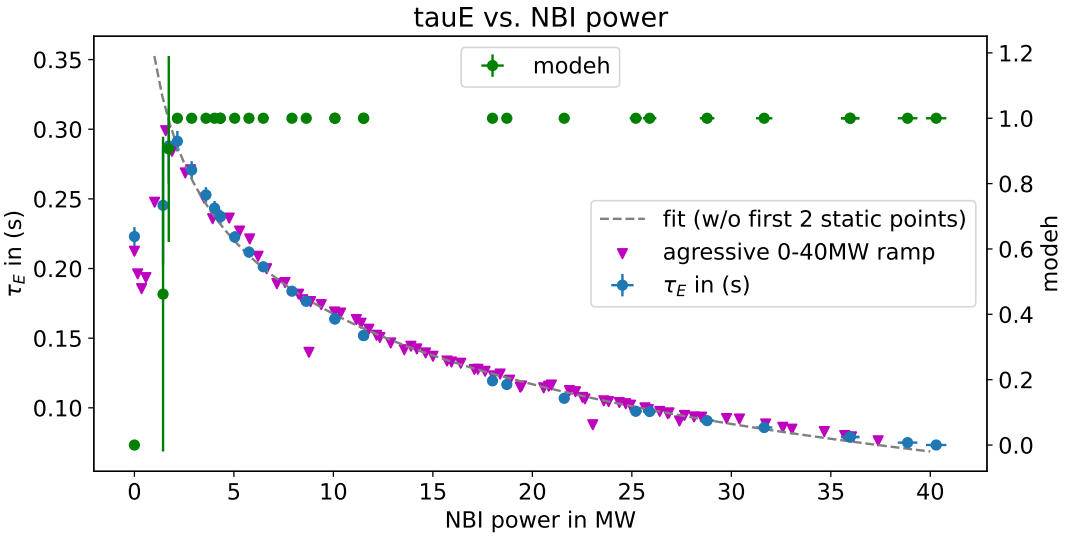

Figure 14: The confinement time against NBI power for the aggressive ramp experiment 5 compared to the static ramp data shown in blue here and taken from figure in section .

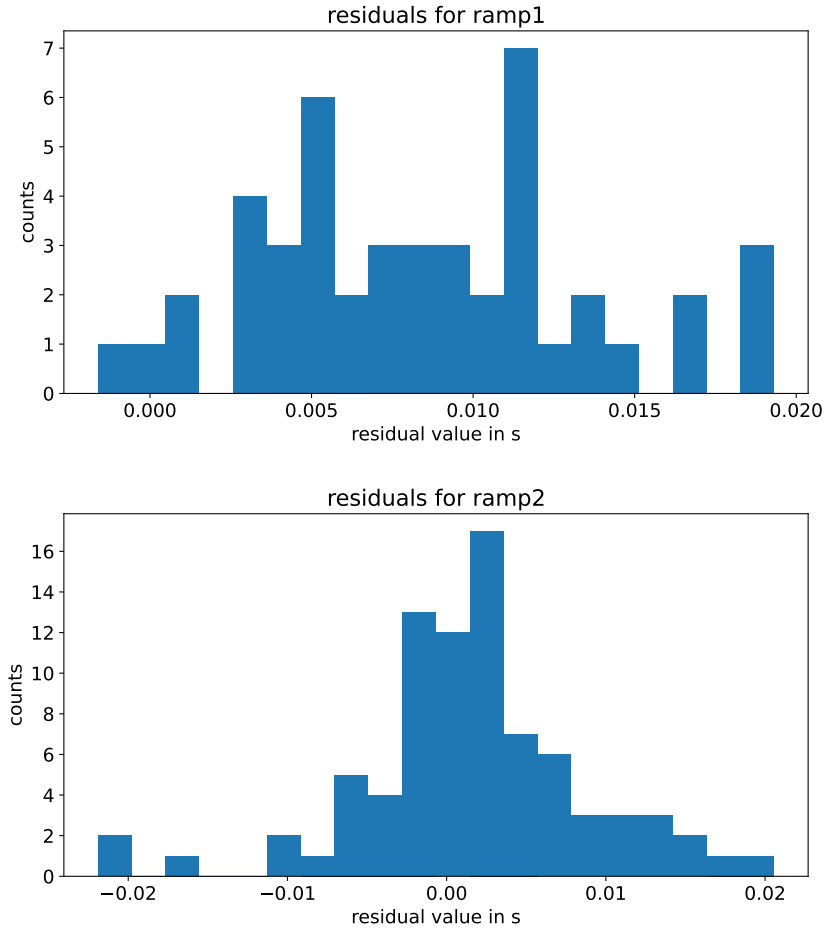

Figure 15: The residuals of the ramp data from the fit based on the static data fro ramp 1 2.

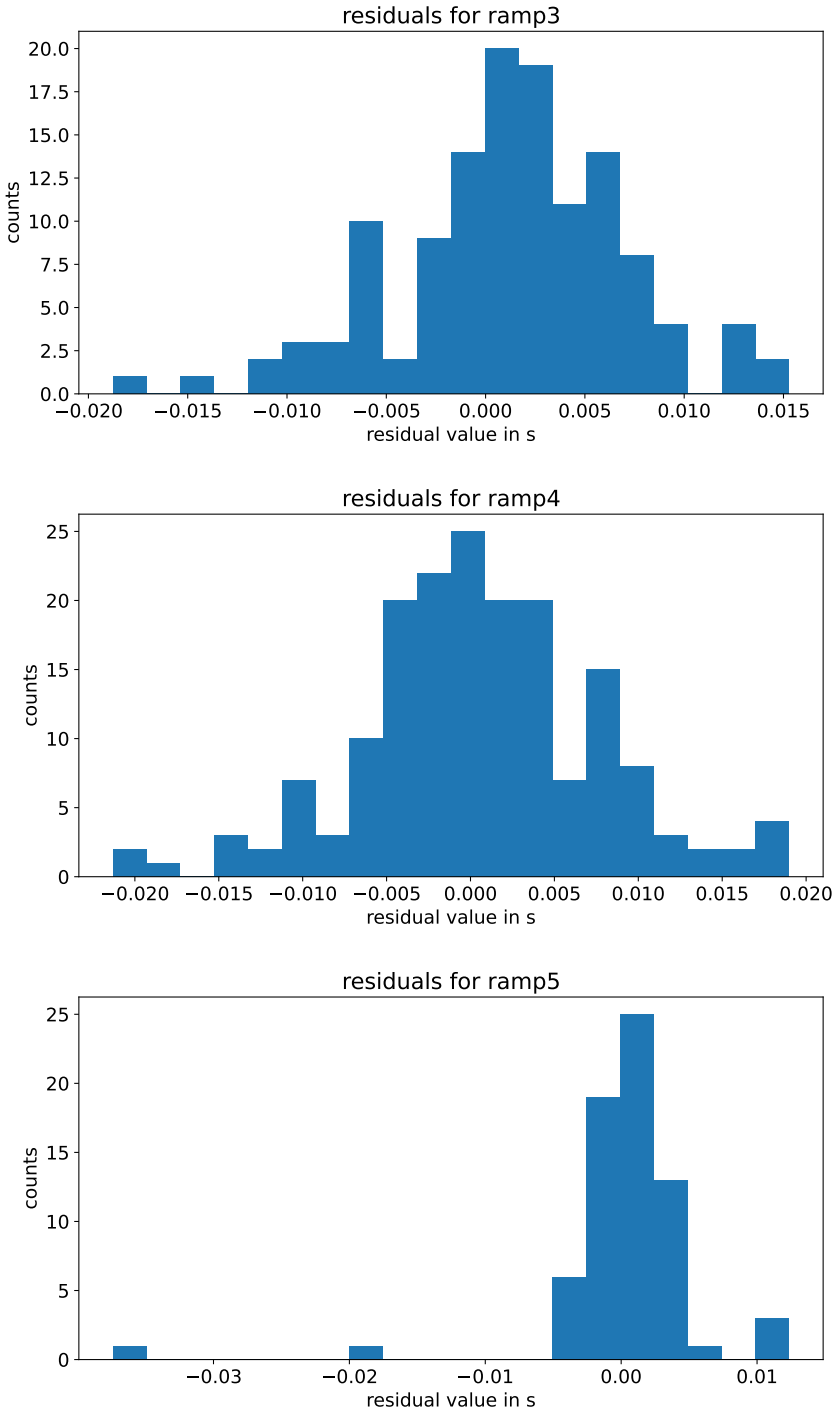

Figure 16: The residuals of the ramp data from the fit based on the static data fro ramp 3,4,5.

4 Optimising triple product

4.1 method

The parameter of the triple product that can be actively controlled is the average density $\overline{n}$. τ_E and T respond to the set parameters. Hence apply the following logic to optimising: Set the density as high as possible as this directly increase the triple product. However all the previous results have shown that the maximum triple product is produced when the plasma is just in H-mode, as the confinement degrades with higher powers. The highest density that can be supported by H-mode is limited by the highest available NBI power as the L-H power threshold increases in density as seen in figure 9.
It should be noted that the threshold can be decreased by decreasing B_t, enabling a higher density for a given NBI power. However, lowering B_t also has limiting effects on the general confinement and hence τ. This trade-off was not explored here and the optimisation was limited to maximising $\overline{n}$ while barely being in H-mode. This approach also eliminates the risk of shine-through of NBI neutrals that comes when optimising through B_t at low densities.
The triple here was read of the graphs in METIS to save time and due to the many simulations that were run.

4.2 results

Increasing the density and adjusting the NBI power accordingly to just reach H-mode gave the results shown in table 1. The maximum achieved triple product shows to be a factor of ~ 3.5 lower than the value that would be required for ignition of $5 \cdot 10^{21}\ keVm^{-3}s^{-1}$ [1, p.13].

density multiplier	NBI power [MW]	triple product $[keVm^{-3}s^{-1}]$
1	2.3	$1.48 \cdot 10^{20}$
4	10.4	$4.75 \cdot 10^{20}$
10	22.3	$8.19 \cdot 10^{20}$
20	38.4	$1.42 \cdot 10^{21}$

Table 1: The triple product as a result of increasing the density while staying in H-mode by increasing the NBI power accordingly.

References

1. Wesson, J. *Tokamaks; 4th ed.* https://cds.cern.ch/record/1427009 (Oxford Univ. Press, Oxford, 2011).
2. Goldston, R. J. Energy confinement scaling in Tokamaks: some implications of recent experiments with Ohmic and strong auxiliary heating. *Plasma Physics and Controlled Fusion* **26,** 87–103. https://doi.org/10.1088/0741-3335/26/1a/308 (Jan. 1984).
3. Greenwald, M. *et al.* H mode confinement in Alcator C-Mod. *Nuclear Fusion* **37,** 793–807. https://doi.org/10.1088/0029-5515/37/6/i07 (June 1997).

4. Freidberg, J. P. *Plasma Physics and Fusion Energy* (Cambridge University Press, 2007).

5. Greenwald, M. Density limits in toroidal plasmas. *Plasma Physics and Controlled Fusion* **44,** R27–R53. https://doi.org/10.1088/0741-3335/44/8/201 (July 2002).

6. Martin, Y. R., Takizuka, T. & the ITPA CDBM H-mode Threshold Data Group. Power requirement for accessing the H-mode in ITER. *Journal of Physics: Conference Series* **123,** 012033. https://doi.org/10.1088/1742-6596/123/1/012033 (July 2008).